Electronic Supplementary Material (ESI) for Journal of Materials Chemistry B.

Supporting Information for

Graphitic-N-doped graphene quantum dots for photothermal eradication of multidrug-resistant bacterial in the second near-infrared window

Bijiang Geng,*[a†] Yuan Li,[b†] Jinyan Hu,[a] Yuanyuan Chen,[b] Junyi Huang,[b] Longxiang Shen,[c] Dengyu Pan*[a] and Ping Li*[b]

[a] School of Environmental and Chemical Engineering, Shanghai University, Shanghai 200444, China.

[b] School of Life Sciences, Shanghai University, Shanghai 200444, China.

[c] Department of Orthopedic Surgery, Shanghai Jiao Tong University affiliated Sixth People's Hospital, Shanghai 200233, China

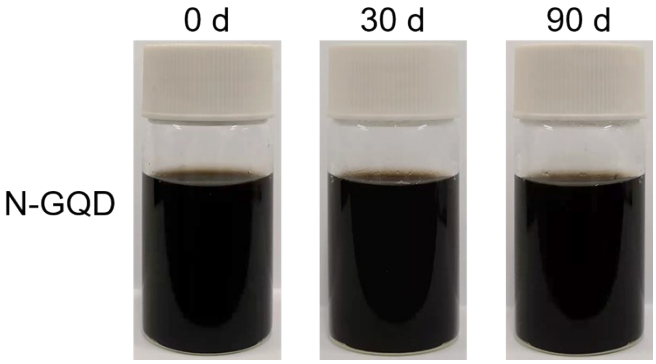

Fig. S1 The photographs of N-GQD solution stored for 90 days.

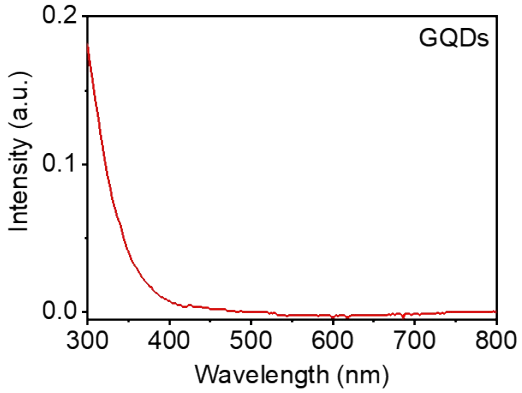

Fig. S2 The absorption spectrum of GQDs without N doped.

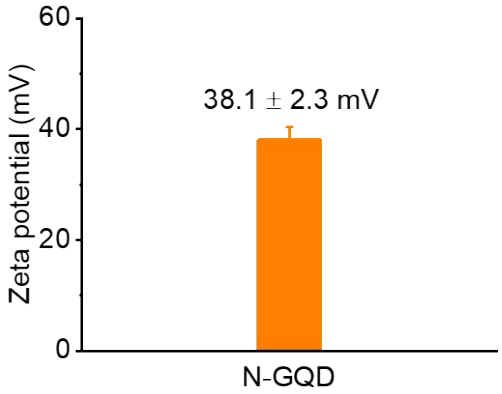

Fig. S3 Zeta potential of N-GQDs (200 μg/mL).

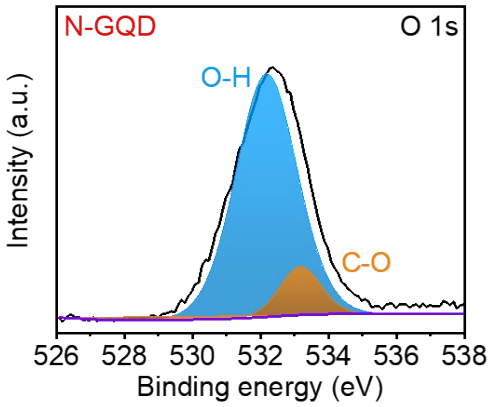

Fig. S4 The high-resolution O 1s spectrum of N-GQDs.

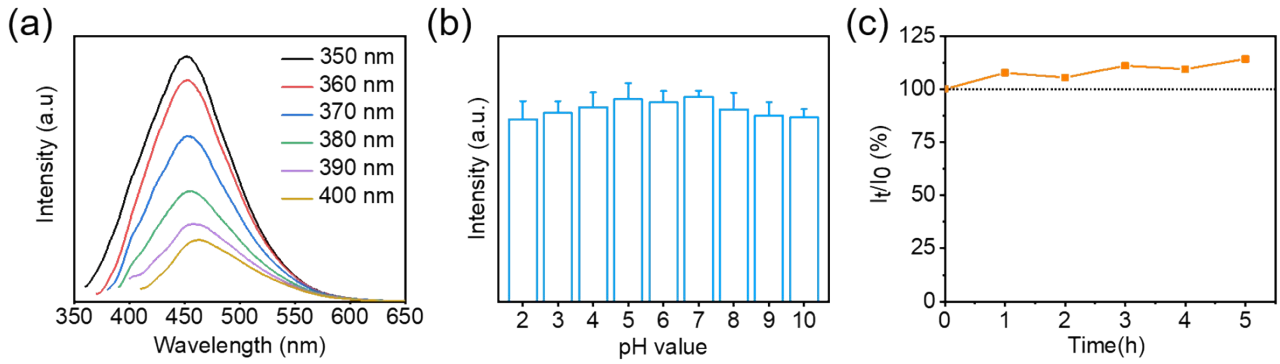

Fig. S5 (a) PL spectra of N-GQDs excited at different wavelengths varied from 350 to 400 nm. (b) Dependence of PL intensity on pH values. (c) Photostability test under 5 h continuous radiation using a 100 W xenon lamp.

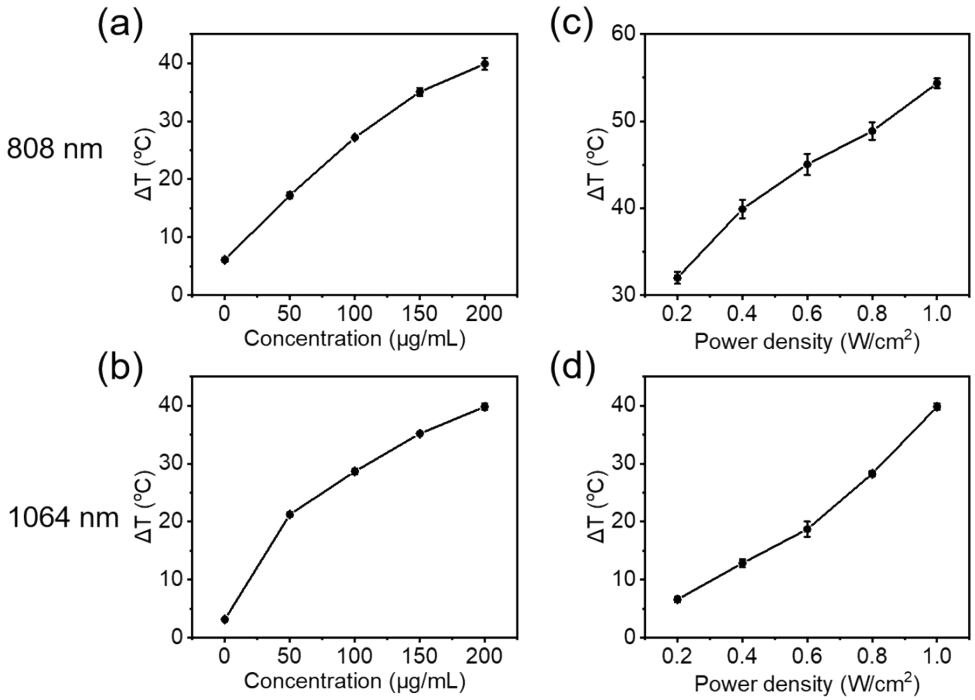

Fig. S6 (a, b) Plot of temperature change (ΔT) over a period of 300 s versus different concentrations of N-GQDs under irradiation with an 808 (a) and 1064 nm (b) laser irradiation at the power density of 0.4 and 1.0 W/cm^2, respectively. (c, d) Plot of temperature change (ΔT) over a period of 300 s versus 808 (c) or 1064 nm (d) laser power density.

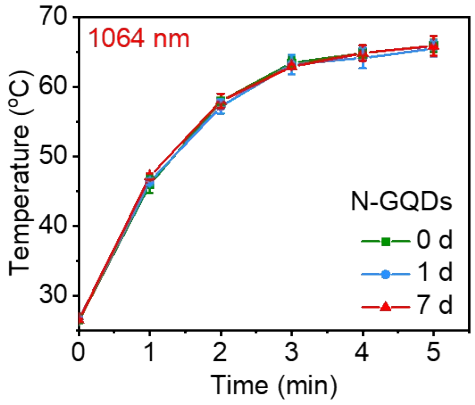

Fig. S7 Temperature elevation of N-GQDs (200 μg/mL) stored for different times (0, 1, and 7 days) under 1064 nm (1.0 W/cm^2) laser irradiation.

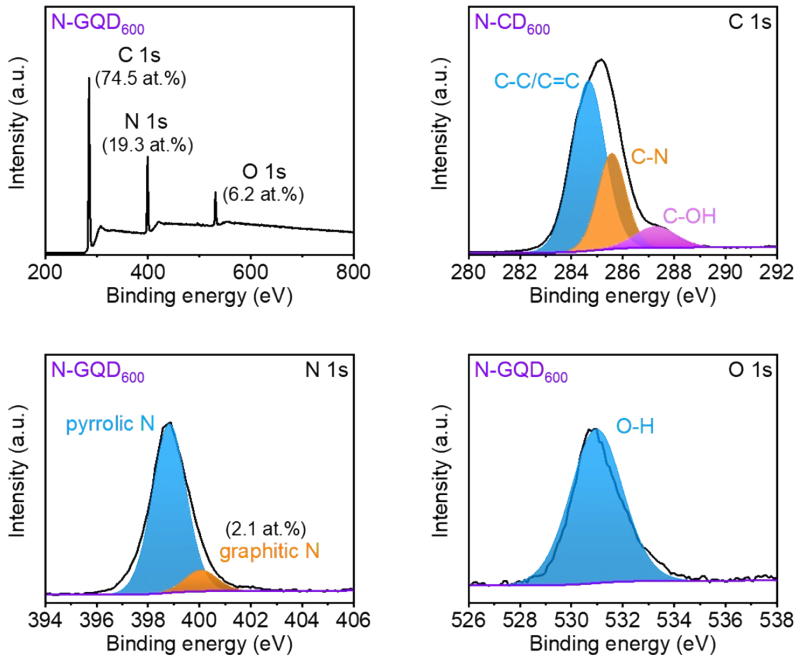

Fig. S8 Survey XPS spectrum, High-resolution C 1s, N 1s, and O 1s spectra of N-GQD$_{600}$.

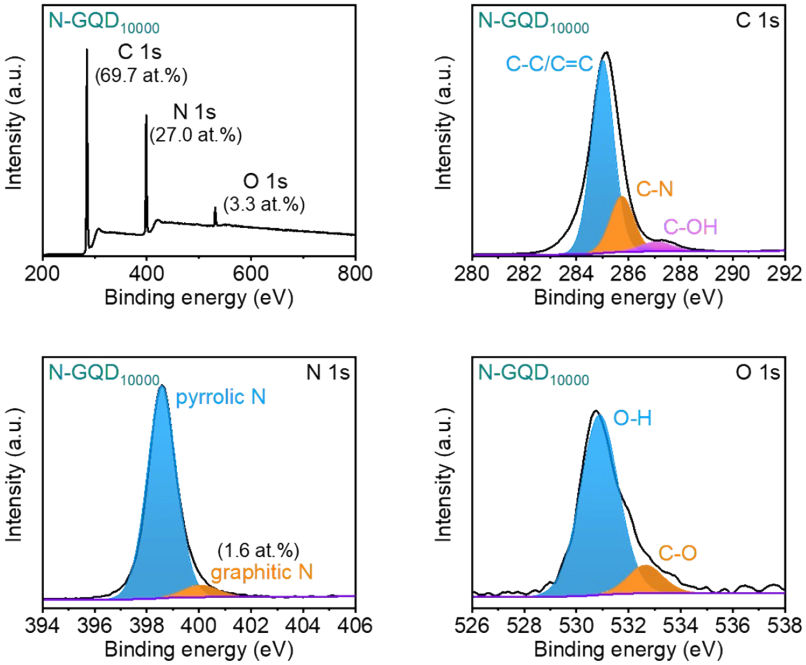

Fig. S9 Survey XPS spectrum, High-resolution C 1s, N 1s, and O 1s spectra of N-GQD$_{10000}$.

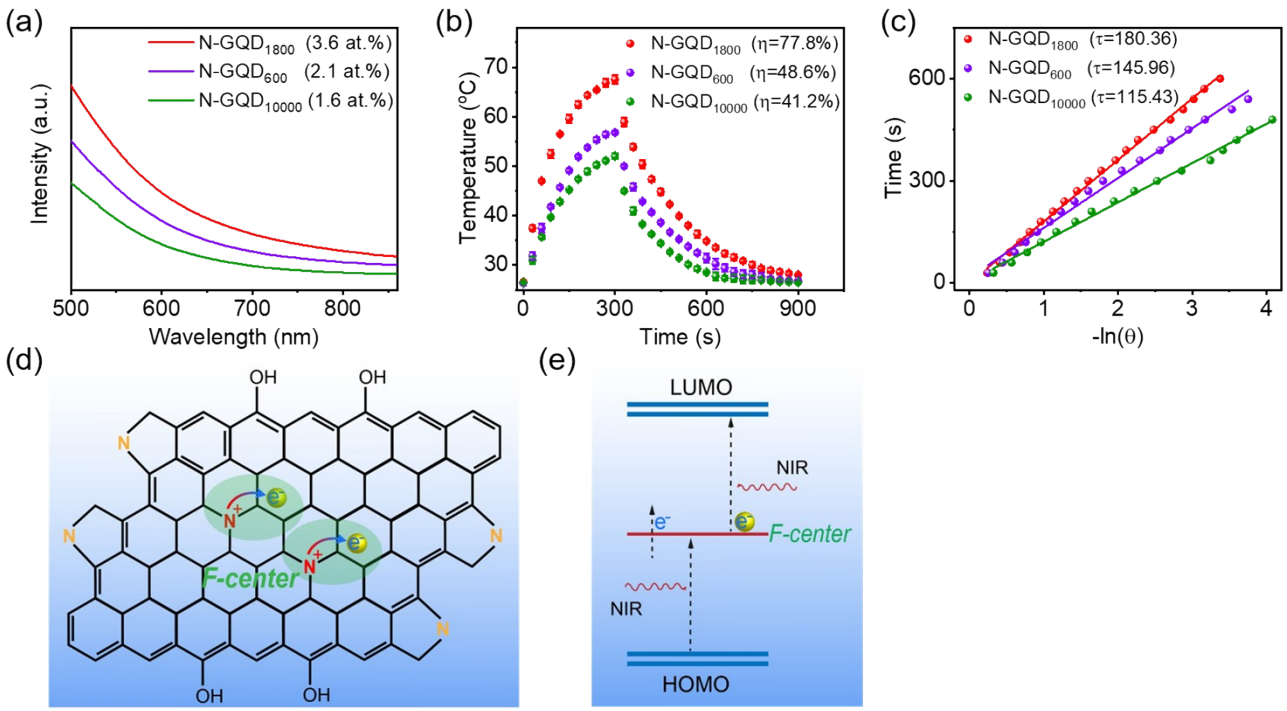

Fig. S10 (a) NIR absorption spectra of three N-GQD samples at the same concentration (200 μg/mL). (b, c) The photothermal conversion efficiency measurements of three N-GQD samples at the same concentration (200 μg/mL). Photothermal effect of the three N-GQD solution exposed to the 808 nm laser at 0.4 W/cm^2. The lasers were shut off after 300 s irradiation. Plot of cooling time versus negative natural logarithm of the temperature driving force obtained from the cooling period after the 808 nm irradiation. (d) Proposed formation mechanism of *F* centers at graphitic N sites, where N atoms donate one excess electron and form N^+ cations to trap the electron with a large binding energy. (e) Defect energy levels of doped graphitic N as a *F* center within the wide band gap of N-GQDs and possible optical transitions from the HOMO level to the defect level and from the singly-occupied defect level to the LUMO level under the NIR excitation.

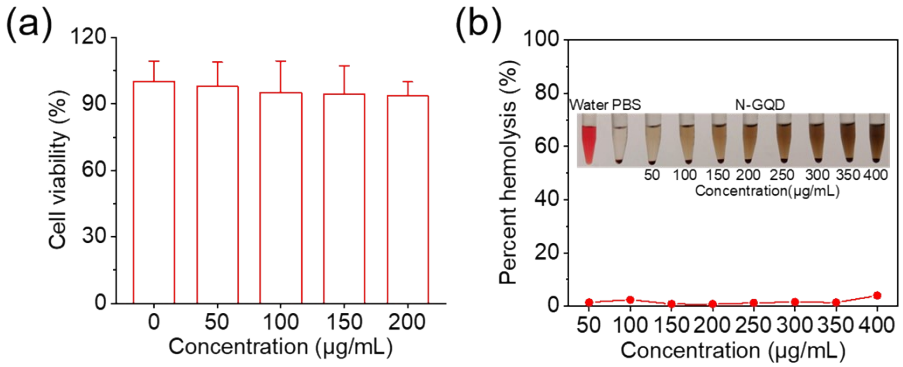

Fig. S11 (a) In vitro cytotoxicity of BEAS-2B cells after receiving treatments with N-GQDs at varied concentrations. (b) Hemolytic percentages of RBCs treated with different concentrations of N-GQD

solution for 3 h.

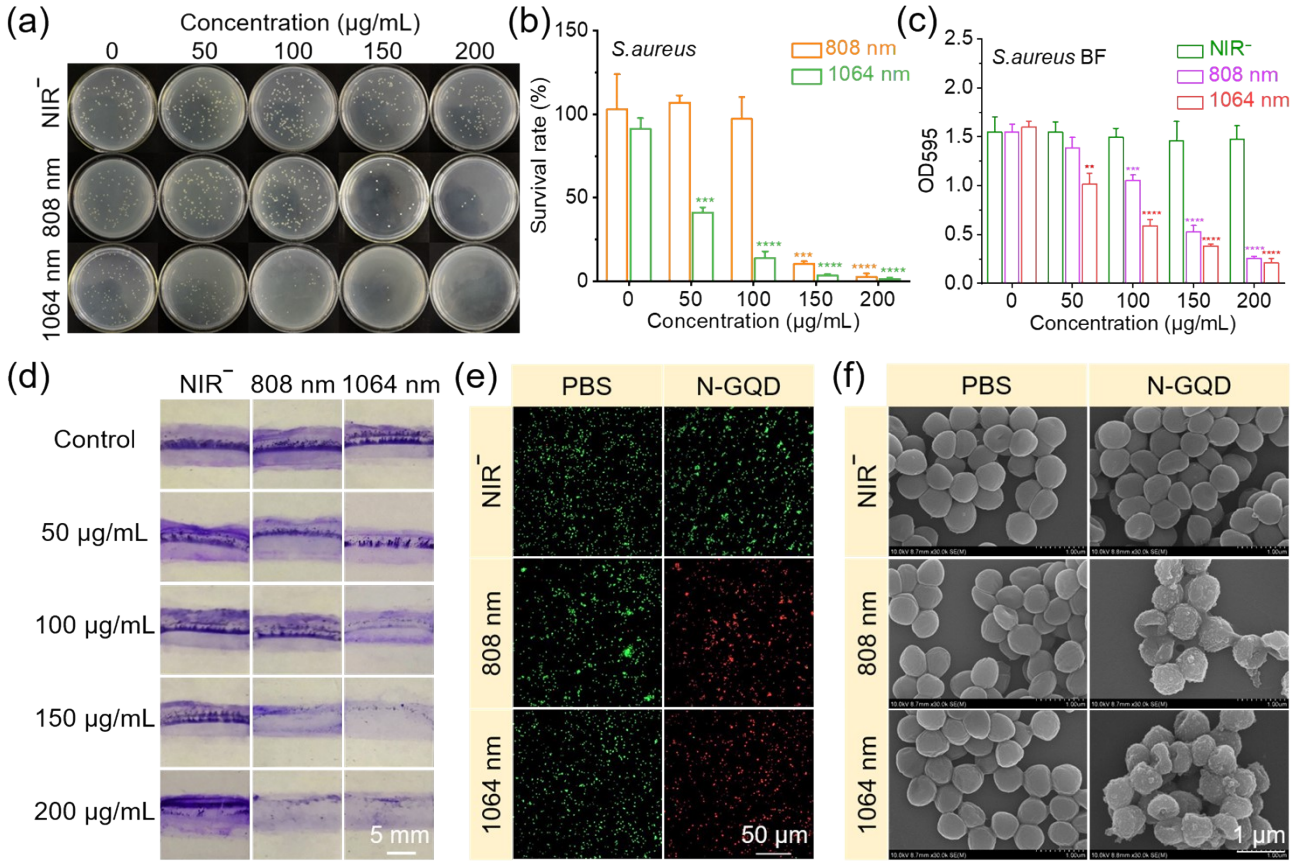

Fig. S12 (a, b) Photographic images of the colonies (a) and the survival rate (b) of *S. aureus* after receiving treatments with varied concentrations of N-GQD aqueous solution without or with 808 (0.4 W/cm^2) or 1064 nm laser (1.0 W/cm^2) irradiation for 5 min. (c) Biomass quantification of *S. aureus* biofilms in (d) by measurement of absorbance at 595 nm. (d) Image of crystal violet staining of *S. aureus* biofilm on glass slides. (e) Live (green fluorescence, SYTO9) and dead (red fluorescence, PI) staining of *S. aureus* under various treatments. (f) SEM images of *S. aureus* after receiving various treatments.

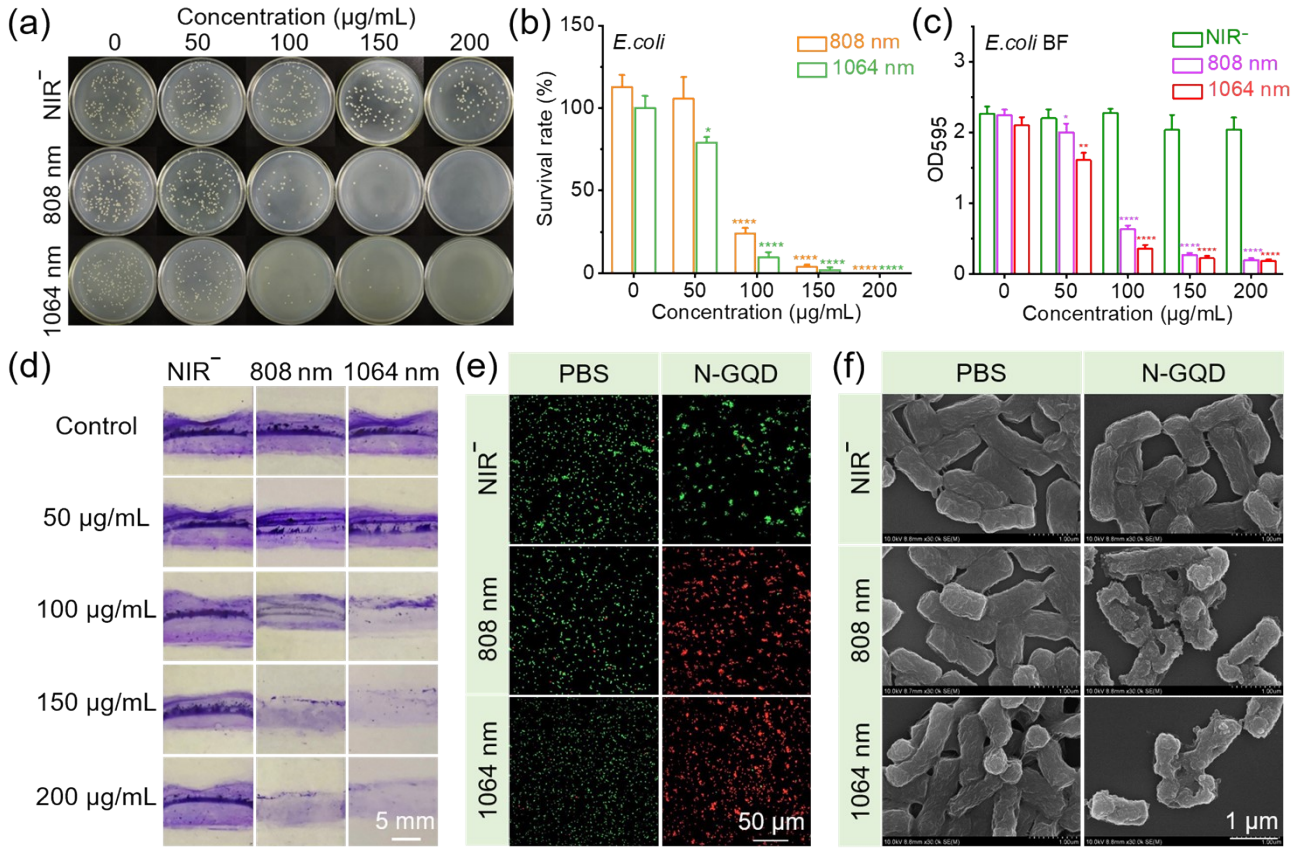

Fig. S13 (a, b) Photographic images of the colonies (a) and the survival rate (b) of *E. coli* after receiving treatments with varied concentrations of N-GQD aqueous solution without or with 808 (0.4 W/cm^2) or 1064 nm laser (1.0 W/cm^2) irradiation for 5 min. (c) Biomass quantification of *E. coli* biofilms in (d) by measurement of absorbance at 595 nm. (d) Image of crystal violet staining of *E. coli* biofilm on glass slides. (e) Live (green fluorescence, SYTO9) and dead (red fluorescence, PI) staining of *E. coli* under various treatments. (f) SEM images of *E. coli* after receiving various treatments.

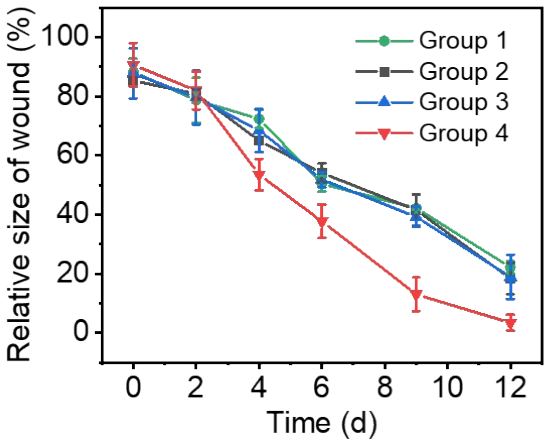

Fig. S14 Wound area from the four groups at different time points during the therapeutic process.

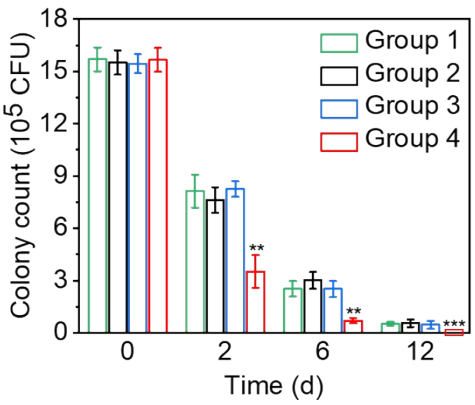

Fig. S15 Statistic analysis of the colony numbers on the LB plate from each group (Group 1: Control; Group 2: NIR; Group 3: N-GQD; Group 4: N-GQD + NIR).

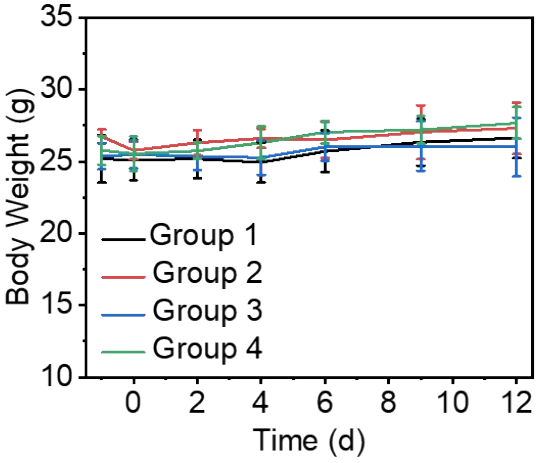

Fig. S16 Body weight of the mice in each group during the therapeutic process.